

Propagations of Fresnel diffraction accelerating beam in Schrödinger equation with nonlocal nonlinearity

Yagang Zhang(张亚港), Yuheng Pei(裴宇恒), Yibo Yuan(袁一博), Feng Wen(闻峰), Yuzong Gu(顾玉宗), and Zhenkun Wu(吴振坤)

Citation: Chin. Phys. B, 2021, 30 (**11**): 114209. DOI: 10.1088/1674-1056/ac068e
Journal homepage: http://cpb.iphy.ac.cn; http://iopscience.iop.org/cpb

What follows is a list of articles you may be interested in

Bound states in the continuum on perfect conducting reflection gratings

Jianfeng Huang(黄剑峰), Qianju Song(宋前举), Peng Hu(胡鹏), Hong Xiang(向红), and Dezhuan Han(韩德专)
Chin. Phys. B, 2021, 30 (**8**): 084211. DOI: 10.1088/1674-1056/abeee4

Three-dimensional spatial multi-point uniform light focusing through scattering media based on feedback wavefront shaping

Fan Yang(杨帆), Yang Zhao(赵杨), Chengchao Xiang(向成超), Qi Feng(冯祺), and Yingchun Ding(丁迎春)
Chin. Phys. B, 2021, 30 (**4**): 044207. DOI: 10.1088/1674-1056/abe3e6

Gain-induced large optical torque in optical twist settings

Genyan Li(李艮艳), Xiao Li(李肖), Lei Zhang(张磊), Jun Chen(陈君)
Chin. Phys. B, 2020, 29 (**8**): 084201. DOI: 10.1088/1674-1056/ab9616

Three-Airy autofocusing beams

Xiao-Hong Zhang(张小红), Fei-Li Wang(王飞利), Lu-Yang Bai(白露阳), Ci-Bo Lou(楼慈波), Yi Liang(梁毅)
Chin. Phys. B, 2020, 29 (**6**): 064204. DOI: 10.1088/1674-1056/ab84d2

Trajectory engineering via a space-fractional Schrödinger equation with dynamic linear index potential

Yunji Meng(孟云吉), Youwen Liu(刘友文), Haijiang Lv(吕海江)
Chin. Phys. B, 2020, 29 (**5**): 054201. DOI: 10.1088/1674-1056/ab7b4c

---

Propagations of Fresnel diffraction accelerating beam in Schrödinger equation with nonlocal nonlinearity*

Yagang Zhang(张亚港)[1], Yuheng Pei(裴宇恒)[2], Yibo Yuan(袁一博)[2], Feng Wen(闻峰)[3], Yuzong Gu(顾玉宗)[1], and Zhenkun Wu(吴振坤)[1,†]

[1] *Institute of Nano/Photon Materials and Application & International Joint Research Laboratory of New Energy Materials and Devices of Henan Province, School of Physics and Electronics, Henan University, Kaifeng* 475004, *China*

[2] *College of Miami, Henan University, Kaifeng* 475004, *China*

[3] *Key Laboratory for Physical Electronics and Devices of the Ministry of Education & School of Science & Shaanxi Key Laboratory of Information Photonic Technique & Institute of Wide Bandgap Semiconductors, Xi'an Jiaotong University, Xi'an* 710049, *China*

(Received 6 May 2021; revised manuscript received 26 May 2021; accepted manuscript online 29 May 2021)

Accelerating beams have been the subject of extensive research in the last few decades because of their self-acceleration and diffraction-free propagation over several Rayleigh lengths. Here, we investigate the propagation dynamics of a Fresnel diffraction beam using the nonlocal nonlinear Schrödinger equation (NNLSE). When a nonlocal nonlinearity is introduced into the linear Schrödinger equation without invoking an external potential, the evolution behaviors of incident Fresnel diffraction beams are modulated regularly, and certain novel phenomena are observed. We show through numerical calculations, under varying degrees of nonlocality, that nonlocality significantly affects the evolution of Fresnel diffraction beams. Further, we briefly discuss the two-dimensional case as the equivalent of the product of two one-dimensional cases. At a critical point, the Airy-like intensity profile oscillates between the first and third quadrants, and the process repeats during propagation to yield an unusual oscillation. Our results are expected to contribute to the understanding of NNLSE and nonlinear optics.

Keywords: Fresnel diffraction beams, nonlocal nonlinearity, real space, momentum space, three-dimensional (3D) Schrödinger equation

PACS: 42.25.Fx, 42.25.Bs, 42.25.Gy **DOI:** 10.1088/1674-1056/ac068e

1. Introduction

Accelerating beams have attracted significant theoretical and experimental research interest in the last few decades owing to their unique features of self-acceleration and diffraction-free propagation over several Rayleigh lengths.[1–8] In particular, Airy beams as exact solutions of the Schrödinger's equation[9,10] indicated that all paraxial accelerated beams are related to the Airy function.[11–17] Until quite recently, study of accelerating beam is still an active topic, and the evolution dynamics of these beams in different medium have been reported in Refs. [18–20]. By applying the separation of variables method to the wave equation and the Helmholtz equation,[21] nonparaxial accelerating beams and Mathieu and Weber beams can be obtained, respectively. Notably, these waves exhibit self-acceleration and self-healing. Additionally, accelerating beams have also been discovered in nonlinear media,[22–24] Bose–Einstein condensates,[25] atomic vapors with electromagnetically induced transparency,[26,27] chiral media,[28] and photonic crystals.[29]

With respect to the propagation dynamics of self-accelerating beams, previous studies have shown that the nonlocality[30,31] and boundary conditions of nonlocal media[32] significantly impact the propagation of solitons. In particular, the spatial properties and anomalous interactions of Airy beams can be modulated considerably via a nonlocal nonlinear potential during propagation.[33–35] Nonlocal optical nonlinearity is observed in nematic liquid crystals[36] and thermal media,[37] where the degree of change induced in the material's refractive index at a specific location is controlled by the light intensity in a specific neighborhood at that location.[38] Nonlocal nonlinearity also affects the interaction of out-of-phase bright solitons and dark solitons.

Motivated by these previous studies, we investigate a self-accelerating beam arising from the paraxial propagation of Fresnel diffraction patterns, which, to the best of our knowledge has not been studied thus far. We first show that this beam exhibits self-acceleration and self-healing, and we then investigate the evolution of these properties — first for the one-dimensional (1D) case involving diffraction at a straight edge, and subsequently for the two-dimensional (2D) case involving diffraction at a corner. We also investigate the periodic inversion and phase transition of Fresnel finite diffraction beams propagating in nonlocal nonlinear media via the fourth-order split-step fast Fourier transform (FFT) method in double precision.[39,40] Through the results of numerical simulations, we conclude that the intensity of the period of the

*Project supported by the National Natural Science Foundation of China (Grant Nos. 61805068, 61875053, and 62074127), China Postdoctoral Science Foundation (Grant No. 2017M620300), and the Fund from the Science and Technology Department of Henan Province, China (Grant No. 202102210111).

†Corresponding author. E-mail: wuzk1121@henu.edu.cn

© 2021 Chinese Physical Society and IOP Publishing Ltd

Fresnel finite diffraction beam is strongly related to the degree of nonlocality. We also show that the nonlocal nonlinear medium exhibits a harmonic potential under a sufficiently high degree of nonlocality, causing the beam to fluctuate in an approximately cosine mode. In the 2D case, the beam undergoes two-phase oscillation and periodic inversion; during propagation, the process repeats, leading to a quasi-periodic breath-like phenomenon during evolution.

2. Theoretical model

2.1. Properties of Fresnel finite diffraction beam

We first consider the 1D case where we generated the Fresnel diffraction of plane waves from a straight edge located at $x = 0$. In this case, the equation describing the normalized amplitude of the Fresnel diffraction pattern can be written as[41]

$$m(x) = \frac{1}{\sqrt{2}}\left[\left(C(x)+\frac{1}{2}\right)+\mathrm{i}\left(S(x)+\frac{1}{2}\right)\right], \tag{1}$$

where

$$C(x) = \int_0^x \cos\left(\frac{\pi}{2}\tau^2\right)\mathrm{d}\tau, \quad S(x) = \int_0^x \sin\left(\frac{\pi}{2}\tau^2\right)\mathrm{d}\tau$$

are the Fresnel cosine and sine integrals, respectively, with $C(\infty) = S(\infty) = 1/2$ and $C(-\infty) = S(-\infty) = -1/2$. However, equation (1) is an ideal equation and is not square-integrable; that is, $\int_{-\infty}^{+\infty}|m(x)|^2\mathrm{d}x \to \infty$. This implies that equation (1) yields infinite energy, which does not exist in reality and can only be described mathematically. For Eq. (1) to be square-integrable, a Gaussian exponential decaying aperture function $\exp(-ax^2)$ can be introduced to enable the convergence of $m(x)$ to a finite energy solution. The modified equation for $m(x)$ with the decay function can be expressed as

$$n(x) = \frac{1}{\sqrt{2}}\left[\left(C(x)+\frac{1}{2}\right)+\mathrm{i}\left(S(x)+\frac{1}{2}\right)\right]\exp\left(-ax^2\right), \tag{2}$$

where $a > 0$ is the attenuation factor associated with the numerical aperture of the system. In Figs. 1(a) and 1(b), we show the diffracting beam intensity distributions and the numerically obtained streaks of $m(x)$ and $n(x)$, respectively. The energy of the propagating beams described by $m(x)$ is infinite, and the oscillating tails of $m(x)$ approach unity as $x \to \infty$. Contrarily, the oscillating tail of the transmitted beam described by $n(x)$ approaches 0 as $x \to \infty$, which leads to a wave packet with finite energy. Moreover, the energy distribution of $n(x)$ is not symmetric under parity and may exhibit acceleration.

The linear Schrödinger equation for the slowly varying envelope of the paraxial wave packet in 1D free space or linear media can be written as

$$\mathrm{i}\frac{\partial\psi}{\partial z}+\frac{1}{2}\frac{\partial^2\psi}{\partial x^2} = 0, \tag{3}$$

where $\psi = n(x)$ is the Fresnel finite diffraction beam envelope. The variable x is the normalized transverse coordinate, and z is the normalized propagation distance — both of which are scaled by a characteristic transverse width x_0 and the corresponding Rayleigh range kx_0^2. Here, $k = 2\pi n/\lambda_0$ is the wavenumber, n is the ambient index of refraction, and λ_0 is the wavelength in free space.[42,43] Figure 1(c) shows the evolution of the finite energy diffraction pattern in a linear medium. As shown by the white dashed curve, it is apparent that the beam accelerates to the left, and the intensity maximum of the beam accelerates during propagation along a parabolic trajectory. All self-accelerating linear beams display the same characteristics: the high-intensity part of the beam is accelerated, while the center of mass of the beam moves along a straight line instead of a parabola.

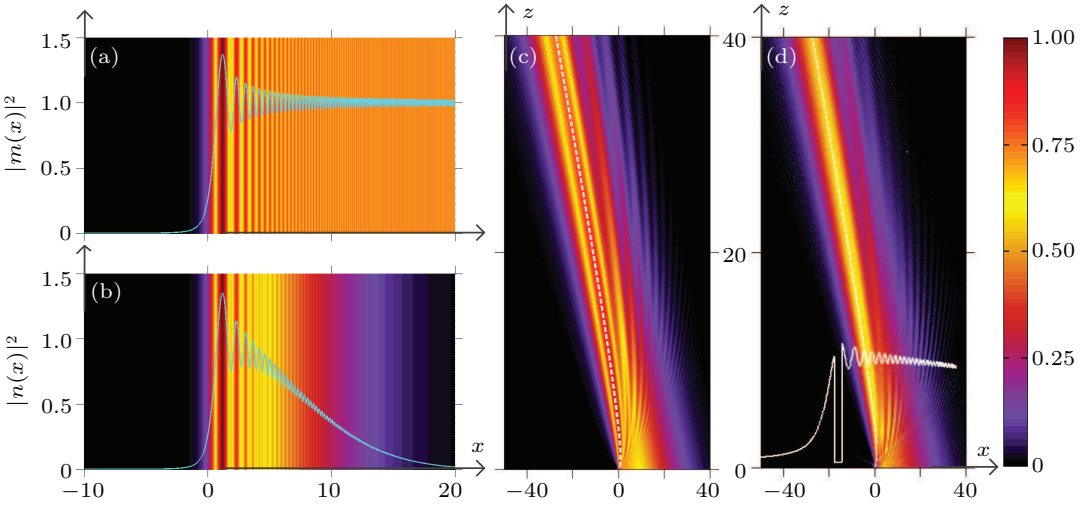


Fig. 1. (a) Intensity $|m(x)|^2$, (b) intensity $|n(x)|^2$, for $a = 0.05$. The background images in panels (a) and (b) depict the ideal and attenuated diffraction patterns. (c) Evolution of $n(x)$ with the theoretical accelerating trajectory indicated by the white dashed curve. (d) The setup is similar to that in panel (c), except for the main lobe being initially cut out.

As shown in Fig. 1(d), the beam evolution indicates the "self-healing" property, and the inset panel represents the energy distribution of the beam at $z = 0$. The main lobe of the beam is screened out initially but recovers quickly with an increase in the propagation distance. This is because energy is transferred from the tail to the head of the beam.

2.2. Dynamics of Fresnel finite diffraction beam in nonlocal nonlinear media

Next, we consider the case of a Fresnel diffraction beam propagating in a nonlocal nonlinear medium because the nonlinear medium has significant effects on the evolution of the beam. In a nonlinear medium, the diffracting beam is described by the following dimensionless nonlocal nonlinear Schrödinger equation (NNLSE):[33]

$$\mathrm{i}\frac{\partial \psi}{\partial z} + \frac{1}{2}\frac{\partial^2 \psi}{\partial x^2} + V(I)\,\psi = 0. \tag{4}$$

Here, the nonlinear expression is

$$V(I) = \int R(x - x')\left|\psi(x', z)\right|^2 \mathrm{d}x',$$

with $R(x)$ corresponding to the normalized symmetrical real nonlocal response function of the medium. To simplify the analysis and render the results more representative and universal, we consider the case of a hyperbolic secant nonlocal response. This means that $R(x) = w\,\mathrm{sech}\left(x/\rho^2\right)$, with the characteristic width ρ representing the degree of nonlocality and w being the characteristic length of the response. Two limiting cases ($\rho \to 0$ and $\rho \to \infty$) are considered, which characterize a local and strongly nonlocal medium, respectively. Although the hyperbolic secant nonlocal response function is phenomenological, it can describe the general properties of actual nonlocal media. In the numerical simulations, the FFT of the convolution term of the nonlinear refractive index change $V(I) = \int R(x - x')\left|\psi(x', z)\right|^2 \mathrm{d}x'$ is expressed as $\mathrm{FFT}\left[V(I)\right] = \mathrm{FFT}\left[R(x)\right] \cdot \mathrm{FFT}\left[\left|\psi(x, z)\right|^2\right]$.

We performed numerical simulations of the propagation of a Fresnel diffraction beam with finite energy in a real space and a momentum space, as shown in Figs. 2(a) and 2(b), respectively. In Fig. 1(c), it can be seen that stationary solitons cannot exist in linear media. However, interestingly, the intensity of the finite energy Fresnel diffraction beam shows periodic repetitions, with the distribution exhibiting opposite bending directions in the region of strong nonlocality, as shown in Fig. 2(a). Specifically, the propagation dynamics exhibit oscillatory properties, which cause the center of mass to oscillate back and forth in the optical axis for a certain period owing to the nonlocality.[44] The distributions of the intensities of these beams exhibit well-defined Airy-like profiles, with the main lobe and a decaying tail. Additionally, there exists a critical point at which the Airy-like beams no longer exhibit multi-peaked profiles, and instead propagate as asymmetric single-peaked beams. This process is repeated during propagation, leading to an unusual oscillation behavior. Moreover, slightly different phenomena are observed in a real space and a momentum space. As shown in Fig. 2(b), when a Fresnel diffracting beam of finite energy evolves from a multi-peaked profile to a single-peaked profile in a real space, it evolves to a decaying tail in a momentum space.

Figures 2(c) and 2(d) show the curves of the peak intensity and the corresponding total power $P = \int \left|\psi(x, z)\right|^2 \mathrm{d}x$ of the beam in a real space and a momentum space as a function of the propagation distance, respectively. It can be seen that the peak intensity of the beam follows a periodic pattern with four sets of maxima over a finite propagation distance, and the peak intensity in a momentum space always lags behind the peak intensity in a real space by half a period. Notably, although the peak intensity decreases gradually with increasing propagation distance, the total power remains approximately constant.[45]

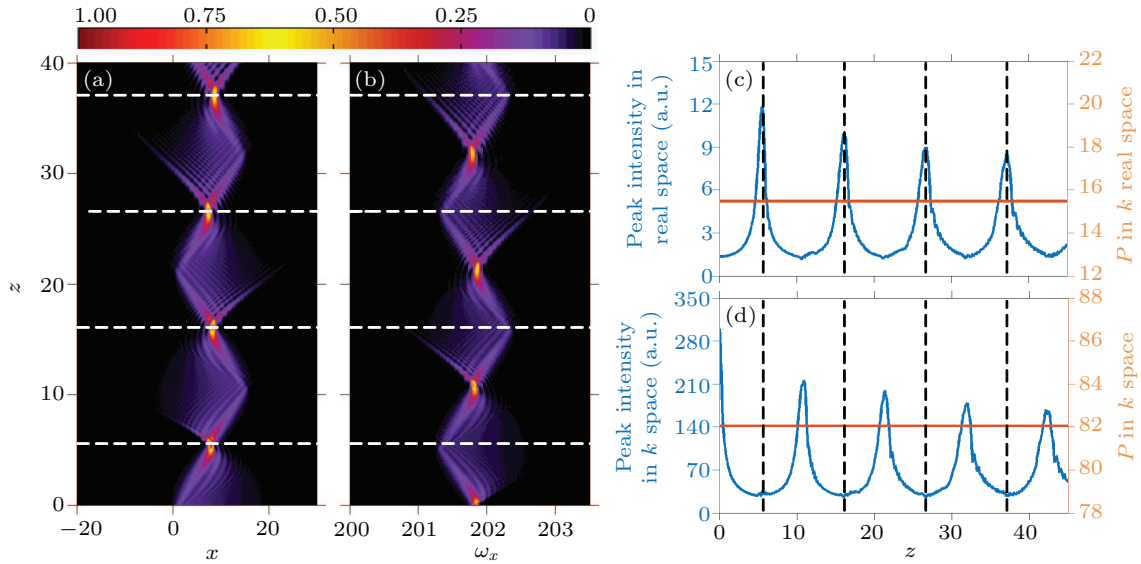


Fig. 2. Propagation intensity patterns of the beam described by Eq. (4): (a) in a real space, and (b) in a momentum space. Peak intensity (blue curves), and total power (orange curves) by propagation distance: (c) in a real space, and (d) in a momentum space. Other parameters are $w = 5$ and $\rho = 5$. The unit a.u. is short for arb. units.

Figures 3(a) and 3(b) show the evolution of the period of a Fresnel diffracting beam for varying degrees of nonlocality in the 1D case. As shown in Fig. 3, the singularity property can also be manifested in the beam propagation dynamics, where the period increases with the degree of nonlocality.[33,46] The reason for this is that the hyperbolic cutline function $R(x) = w\,\mathrm{sech}\left(x/\rho^2\right)$ is reduced to a parabolic potential when the degree of nonlocality ρ is sufficiently large. Therefore, it is difficult to bind the Fresnel diffraction beam of finite energy into solitons under the condition of strong nonlocality. It is worth noting that in addition to nonlocal nonlinear media, bent space and photonic lattices also display similar propagation properties of periodic intensity-distributed beams with opposite bending directions.

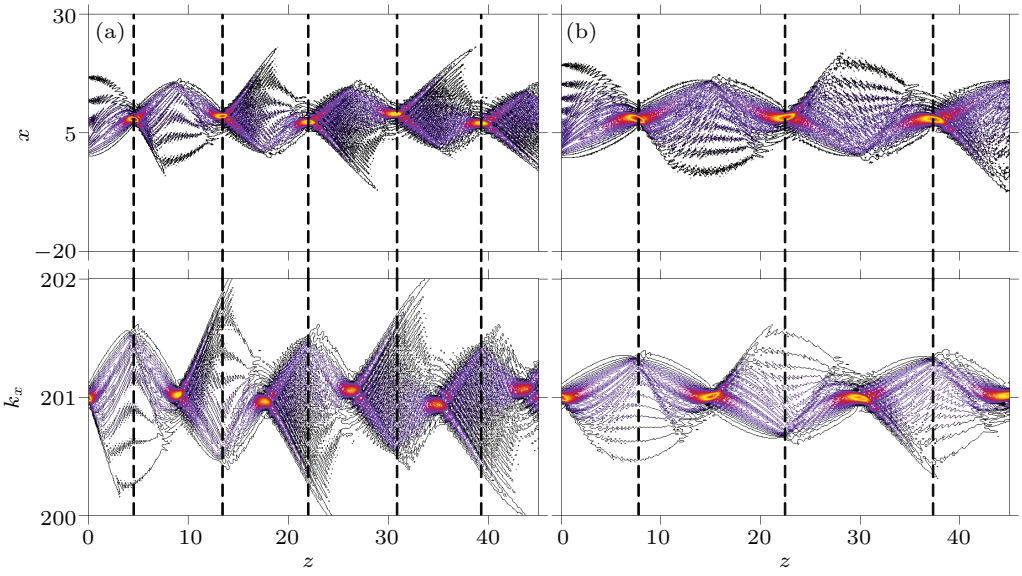


Fig. 3. Evolution intensity contour lines patterns of finite-energy Fresnel diffraction beams according to Eq. (4) in real space and momentum space with different degrees of nonlocality. The parameters are the same as those in Fig. 2, with (a) $\rho = 3$ and (b) $\rho = 8$.

3. Two-dimensional case

Next, we extend the Fresnel diffracted beam from one to two dimensions and analyze the properties of the diffracted beam in the 2D case. Our analysis shows that the beam is diffracted from a right angle located at the origin of the Cartesian coordinate system $(x = 0, y = 0)$. The normalized equation describing the amplitude for the Fresnel diffraction pattern can be written as

$$M(x,y) = \frac{1}{2}\left[\left(C(x)+\frac{1}{2}\right)+\mathrm{i}\left(S(x)+\frac{1}{2}\right)\right] \times \left[\left(C(y)+\frac{1}{2}\right)+\mathrm{i}\left(S(y)+\frac{1}{2}\right)\right]. \quad (5)$$

Similarly, repeating the operations in Eqs. (1) and (2), we introduce a Gaussian exponential decaying aperture to enable the beam to converge to finite energy. Thus, equation (5) is transformed into

$$N(x,y) = M(x,y)\exp\left[-a\left(x^2+y^2\right)\right]. \quad (6)$$

From Fig. 4(a), it is clear that the ideal 2D diffraction pattern based on Eq. (5) is not square-integrable, thereby yielding infinite energy. However, equation (6), which includes a Gaussian aperture function, has finite energy, as presented in Fig. 4(b). Furthermore, by utilizing the Lorentz transformation of coordinates, the right-angle corner diffraction can be easily generalized to a 2D acute- or obtuse-angle Fresnel diffraction. In particular, when the angle of the corner is greater than π, the diffraction can be regarded as that from the corner of a wedge-shaped angle, and the analytical expression for an ideal diffraction pattern can be written as

$$M(x,y) = \frac{1}{2}\left[\left(C(x)+\frac{1}{2}\right)+\mathrm{i}\left(S(x)+\frac{1}{2}\right)\right] \times \left[\left(C(y)+\frac{1}{2}\right)+\mathrm{i}\left(S(y)+\frac{1}{2}\right)\right] + \frac{1}{2}\left[\left(C(-x)+\frac{1}{2}\right)+\mathrm{i}\left(S(-x)+\frac{1}{2}\right)\right] \times \left[\left(C(-y)+\frac{1}{2}\right)+\mathrm{i}\left(S(-y)+\frac{1}{2}\right)\right]. \quad (7)$$

Based on this formula and the Lorentz transformation,[47] the 2D Fresnel diffraction pattern from a wedge with an angle $0 < \theta < \pi$ can be obtained. In Figs. 4(c) and 4(d), we show the infinite and finite diffraction patterns with $\theta = \pi/2$, respectively.

Concurrently, the Fresnel diffracting beams with finite energy in a 2D nonlocal nonlinear medium exhibit equally interesting properties, including (but not limited to) characteristic periodic reversals and phase transitions in the propagation dynamics. According to the analysis presented in Ref. [48], this periodic behavior can be attributed to the linearity of the problem. The extension from 1D to 2D can be realized naturally, as the 2D case can be considered to be the product of two

1D cases. For the 2D propagation of a finite-energy Fresnel diffraction beam in the nonlocal nonlinear media, equation (4) should be modified as

$$\mathrm{i}\frac{\partial \psi}{\partial z}+\frac{1}{2}\left(\frac{\partial^2 \psi}{\partial x^2}+\frac{\partial^2 \psi}{\partial y^2}\right)+V\left[I(x,y)\right]\psi=0. \tag{8}$$

The nonlinear perturbation is given by the following equation:

$$V\left[I(x,y)\right]=\iint R\left(r-r'\right)\left|\psi\left(x',y',z\right)\right|^2 \mathrm{d}x'\,\mathrm{d}y'. \tag{9}$$

In Eq. (9), the 2D hyperbolic secant nonlocal response function is given by $R(x,y)=w\,\mathrm{sech}\left(x/\sigma^2\right)\mathrm{sech}\left(y/\sigma^2\right)$. The solutions of Eq. (8) can be easily calculated by using the inverse scattering transform, whose solutions are related to the Hermite, Bessel, or Airy functions. In this section, we describe the propagation dynamics of a 2D finite-energy Fresnel diffracting beam in a nonlocal nonlinear medium by numerically integrating Eq. (8), using Eq. (6) as a reference.

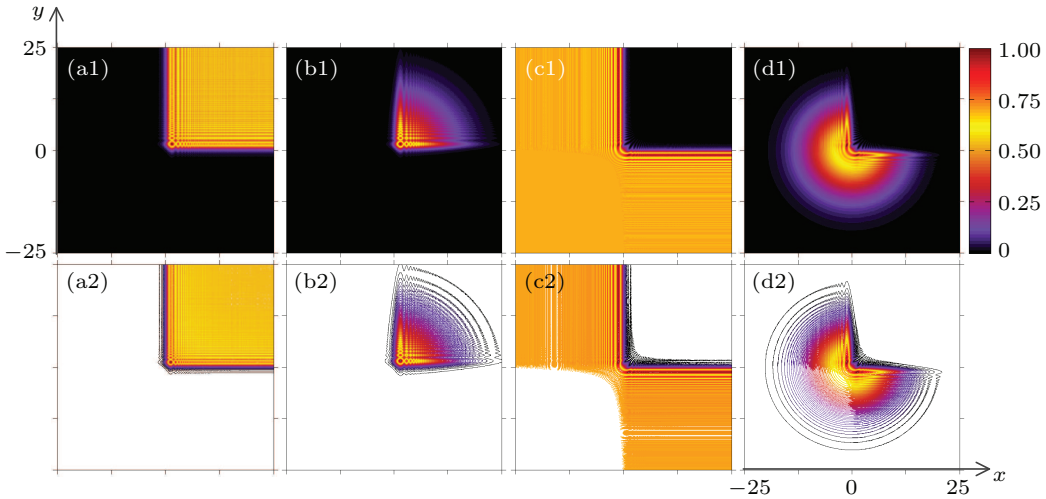


Fig. 4. Panels (a1) and (b1) are Fresnel infinite and finite diffraction patterns at a right-angled corner, respectively. Panels (c1) and (d1) are Fresnel infinite and finite diffraction patterns from a wedge with angle $\theta=\pi/2$, respectively. The bottom panel shows the intensity contour lines patterns corresponding to the top panel. The decay factor is $a=0.05$.

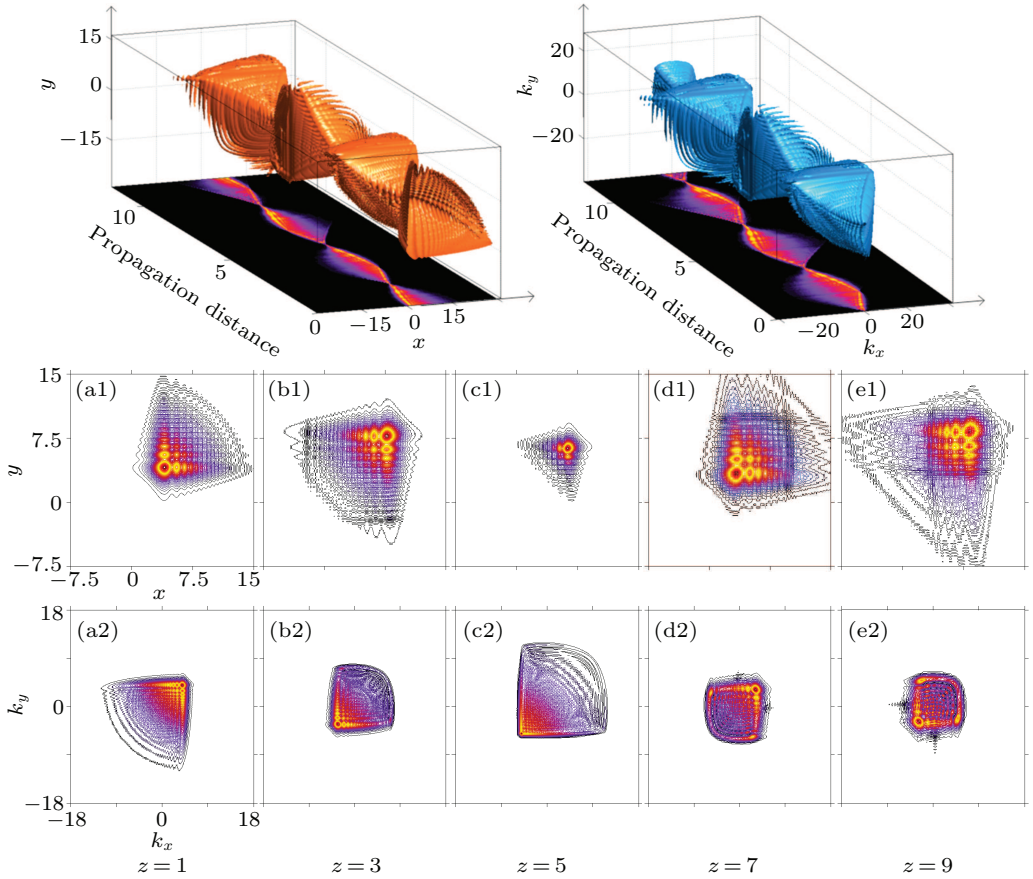


Fig. 5. Propagation of a 2D finite-energy Fresnel diffraction beam in nonlocal nonlinear media. Top panel: Iso-surface plot of the intensity during propagation. Panels (a1)–(e1) and (a2)–(e2) are intensity contour line patterns in a real space and a momentum space, respectively, when the beam propagates from $z=1$, 3, 5, 7, and 9. The other parameters are $w=10$ and $\rho=5$.

As shown in Fig. 5, the three-dimensional (3D) surface plot in the top panel depicts that the beam undergoes two-phase oscillations and a periodic inversion. In real space, the spatial intensity distribution of the beam decreases at first and subsequently increases. This process is repeated during propagation, thereby resulting in a quasi-periodic breath-like phenomenon in the evolution. However, in momentum space, the opposite process occurs, with the spatial intensity distribution tending to first increase and then decrease. As described before, in the case of the 2D cross-section, the intensity distribution changes in the real and momentum spaces in the opposite manner.

The oscillation process can be better understood in the projection of the 3D graph, similar to the cases in Figs. 2 and 3. To further explore the phase transition, we show the intensity distribution of the beam at specific distances in Figs. 5(a)–5(e), where the intensity snapshots are adopted from the same simulation at propagation distances $z = 1$, 3, 5, 7, and 9, respectively. It can be seen that the Airy-like intensity distribution oscillates between the first and third quadrants. Due to the finite energy, the 2D cross-section of the beam expands or contracts periodically within a limited range as the propagation distance increases.

4. Conclusion

In this study, we have theoretically and numerically demonstrated the propagation dynamics of finite-energy Fresnel diffraction beam in linear and nonlocal nonlinear media. In one dimension, we find that the finite-energy Fresnel diffraction beam accelerates to the left, and self-healing evolution occurs after a small barrier during linear propagation of the beam. In contrast, in the nonlocal nonlinear medium, the propagation dynamics of the 1D finite-energy Fresnel diffraction beam exhibit anomalous oscillation properties, causing the centroid to oscillate back and forth with certain periods across the optical axis, owing to the nonlocality. As the degree of nonlocality increases, the period becomes larger but the intensities of the beams always maintain an Airy-like profile, with the main lobe and a decaying tail. Additionally, we investigate the propagation of Fresnel diffraction from a corner of a different angle when the beam propagates in the 2D nonlinear medium. In particular, the Airy-like intensity profile oscillates between the first and third quadrants, and the process repeats during propagation, resulting in unique oscillations. Overall, our results not only demonstrate a novel accelerating beam but also contribute to the understanding of NNLSE and nonlinear optics.

References

[1] Siviloglou G A and Christodoulides D N 2007 *Opt. Lett.* **32** 979
[2] Siviloglou G A, Broky J, Dogariu A and Christodoulides D N 2007 *Phys. Rev. Lett.* **99** 213901
[3] Broky J, Siviloglou G A, Dogariu A and Christodoulides D N 2008 *Opt. Express* **16** 12880
[4] Ellenbogen T, Voloch-Bloch N, GananyPadowicz A and Arie A 2009 *Nat. Photon.* **3** 395
[5] Chong A, Renninger W H, Christodoulides D N and Wise F W 2010 *Nat. Photon.* **4** 103
[6] Zhou J X, Liu Y H, Ke Y G, Luo H L and Wen S C 2015 *Opt. Lett.* **40** 3193
[7] Wu W J, Zhang W S, Chen S Z, Ling X H, Shu W X, Luo H L, Wen S C and Yin X B 2018 *Opt. Express* **26** 23705
[8] Xu D Y, He S S, Zhou J X, Chen S Z, Wen S C and Luo H L 2020 *Opt. Lett.* **45** 6867
[9] Berry M V and Balazs N L 1979 *Am. J. Phys.* **47** 264
[10] Lin C L, Hsiung T C and Huang M J 2008 *Europhys. Lett.* **83** 30002
[11] Durnin J 1987 *J. Opt. Soc. Am. A* **4** 651
[12] Bouchal Z 2003 *Czech. J. Phys.* **53** 537
[13] Wu Z K and Gu Y Z 2019 *Commun. Theor. Phys.* **71** 741
[14] Chen Y H, Wu L X, Mo Z X, Wu L C and Deng D M 2021 *Chin. Phys. B* **30** 014204
[15] He S L, Malomed B A, Mihalache D, Peng X, Yu X, He Y J and Deng D M 2021 *Chaos, Solitons and Fractals* **142** 110470
[16] Liu X Y, Sun C and Deng D M 2021 *Chin. Phys. B* **30** 024202
[17] Chen B, Chen C D, Peng X, Peng Y L, Zhou M L, Deng D M and Guo H 2016 *J. Opt.* **18** 055504
[18] Zhang X H, Wang F L, Bai L Y, Lou C B and Liang Y 2020 *Chin. Phys. B* **29** 064204
[19] Zhu Y F and Geng T 2020 *Acta Phys. Sin.* **69** 014205 (in Chinese)
[20] Chen X P, Xu C J, Yang Q, Luo Z M, Li X X and Deng D M 2020 *Chin. Phys. B* **29** 064202
[21] Zhang P, Hu Y, Li T, Cannan D, Yin X, Morandotti R, Chen Z and Zhang X 2012 *Phys. Rev. Lett.* **109** 193901
[22] Kaminer I, Segev M and Christodoulides D N 2011 *Phys. Rev. Lett.* **106** 213903
[23] Lotti A, Faccio D, Couairon A, Papazoglou D G, Panagiotopoulos P, Abdollahpour D and Tzortzakis S 2011 *Phys. Rev. A* **84** 021807
[24] Panagiotopoulos P, Abdollahpour D, Lotti A, Couairon A, Faccio D, Papazoglou D G and Tzortzakis S 2012 *Phys. Rev. A* **86** 013842
[25] Efremidis N K, Paltoglou V and von Klitzing W 2013 *Phys. Rev. A* **87** 043637
[26] Zhuang F, Shen J, Du X and Zhao D 2012 *Opt. Lett.* **37** 3054
[27] Ru J M, Wu Z K, Zhang Y G, Wen F and Gu Y Z 2020 *Front. Phys.* **15** 52503
[28] Zhuang F, Du X, Ye Y and Zhao D 2012 *Opt. Lett.* **37** 1871
[29] Kaminer I, Nemirovsky J, Makris K G and Segev M 2013 *Opt. Express* **21** 8886
[30] Kong Q, Wang Q, Bang O and Krolikowski W 2010 *Phys. Rev. A* **82** 013826
[31] Hu W, Zhang T and Guo Q 2006 *Appl. Phys. Lett.* **89** 071111
[32] Bekenstein R and Segev M 2011 *Opt. Express* **19** 23706
[33] Wu Z K, Wang Z P, Guo H and Gu Y Z 2017 *Opt. Express* **25** 30468
[34] Zhou G Q, Chen R P and Ru G Y 2014 *Laser Phys. Lett.* **11** 105001
[35] Bekenstein R, Schley R, Mutzafi M, Rotschild C and Segev M 2015 *Nat. Phys.* **11** 872
[36] Peccianti M, Conti C, Assanto G, De Luca A and Umeton C 2004 *Nature* **432** 733
[37] Rotschild C, Alfassi B, Cohen O and Segev M 2006 *Nat. Phys.* **2** 769
[38] Wu Z K, Li P, Zhang Y B, Guo H and Gu Y Z 2019 *J. Opt.* **21** 105602
[39] Xu X M and Taha T 2003 *J. Math. Model. Algorithms* **2** 185
[40] Muslu G M and Erbay H A 2005 *Math. Comput. Simulat.* **67** 581
[41] Zhang Y Q, Belić M R, Zheng H B, Wu Z K, Li Y Y, Lu K Q and Zhang Y P 2013 *Europhys. Lett.* **104** 34007
[42] Zhang Y Q, Belić M R, Zheng H B, Chen H X, Li C B, Li Y Y and Zhang Y P 2014 *Opt. Express* **22** 7160
[43] Zhang Y Q, Belić M R, Wu Z K, Zheng H B, Lu K Q, Li Y Y and Zhang Y P 2013 *Opt. Lett.* **38** 4585
[44] Zhang Y Q, Liu X, Belić M R, Zhong W P, Zhang Y P and Xiao M 2015 *Phys. Rev. Lett.* **115** 180403
[45] Wu Z K, Zhang Y G, Ru J M and Gu Y Z 2020 *Results Phys.* **16** 103008
[46] Zhang Y G, Wu Z K, Ru J M, Wen F and Gu Y Z 2020 *J. Opt. Soc. A B* **37** 3414
[47] Eichelkraut T J, Siviloglou G A, Besieris I M and Christodoulides D N 2010 *Opt. Lett.* **35** 3655
[48] Wu Z K, Li P and Gu Y Z 2016 *Front. Phys.* **12** 124203